ISTITUTO NAZIONALE
DI OCEANOGRAFIA E DI GEOFISICA SPERIMENTALE

**Bollettino di Geofisica
Teorica ed Applicata**

Trieste July 2, 2015

Dr Milena Menna
OGS
Borgo GRotta Gigante 42c
34010 Sgonico (TS)

Subject: BGTA paper

Dear dr Menna,

I am glad to inform you that your paper

Upwelling features off the Northwest Africa coast in 2009-2013

by Milena Menna, Saliou Faye, Pierre-Marie Poulain, Luca Centurioni, Alban Lazar, Amadou Gaye, Bamol Sow, Dominique Dagorne

has been accepted for publication in the "Bollettino di Geofisica Teorica ed Applicata".

Many thanks for your co-operation and best regards.

Yours sincerely,

Dario Slejko
Publishing Editor del BGTA
Ist. Naz. Oceanografia e Geofisica Sperimantale
Borgo Grotta Gigante 42c
34010 SGONICO (TS)

Borgo Grotta Gigante 42/c
34010 Sgonico (Trieste)
Tel. +39 040 21401
Fax +39 040 327307
Cod. Fisc. e Partita IVA: 00055590327
CEE IT 00055590327
E-mail: mailbox@ogs.trieste.it
http://www.ogs.trieste.it

Upwelling features off the Northwest Africa coast in 2009-2013

Milena Menna[a] (mmenna@ogs.trieste.it), Saliou Faye[b,e] (fayebayzal100@yahoo.fr), Pierre-Marie Poulain[a] (ppoulain@ogs.trieste.it), Luca Centurioni[c] (lcenturioni@ucsd.edu), Alban Lazar[d,e] (alban.lazar@locean-ipsl.upmc.fr), Amadou Gaye[e] (atgaye@ucad.sn), Bamol Sow[f,e] (bsow@univ-zig.sn), Dominique Dagorne[g] (dominique.dagorne@ird.fr)

[a] Istituto di Oceanografia e Geofisica Sperimentale - OGS, Sgonico (TS), Italy.
[b] Centre de Recherches Océanographiques Dakar-Thiaroye (CRODT), Dakar, Sénégal
[c] Scripps Institution of Oceanography, UCSD, La Jolla, California
[d] CNRS/IRD, Paris, France
[e] LPAOF/UCAD, Dakar, Senegal
[f] Université de Ziguinchor, Ziguinchor, Sénégal
[g] Institute de Recherche pour le Développement, US Imago, BP70, F-29280 Plouzané, France

Corresponding author: Milena Menna; mmenna@ogs.trieste.it; OGS, Borgo Grotta Gigante, 42/c, 34010 Sgonico (TS), Italy; telephone: +39 3383019108; fax: +39 040327307

Abstract

Satellite data (images of sea surface temperature and chlorophyll-a), ocean surface wind products, Lagrangian observations (surface drifters) and other ancillary data (upwelling index) are used to describe the upwelling seasons off northwest Africa during 2009-2013, with particular focus on the Senegal and Mauritania coasts. The impact of the upwelling is characterised by a comparative analysis, carried out in terms of wind-induced upwelling and water/ecosystem response to this forcing, between five geographical sectors detected in the study area. The wind forcing analysis shows the most favourable upwelling conditions in the period December-June in the southern sectors (south of 16°N), and from February to October in the northern sectors (north of 18°N). Southern sectors are strongly influenced by wind forcing, whereas to the north the upwelling occurs also during the months with low Ekman transport values. The analysis of the sea surface temperature and chlorophyll-a concentration confirms the existence of an upwelling season during winter-spring in the south, and emphasizes the different behaviors between the northern and southern sectors. Drifter tracks allow to add some details about the flow of cold water offshore and alongshore. In particular, they describe the westward transport of cold water, by means of energetic filaments rooted at specific locations along the coast, north of Cape Vert and the south-southwestward transport of the coastal water south of Cap Vert.

1. Introduction

The Canary Current Upwelling System (CCUS), that extends from the Iberian Peninsula (43°N) to the south of Senegal (8°N), is one of the four major eastern boundary upwelling regions of the

world ocean (Santos et al., 2005; Aristegui et al., 2009; Benazzouz, 2014) and sustains large fisheries resources (Marchesiello et al., 2004). Upwelling events in this region are triggered by the northeasterly along-shore Trade winds, that drive the surface Ekman transport offshore. The strength of the winds is modulated by the seasonal migration of the Intertropical Convergence Zone and of the Azores high-pressure cell (Wooster et al., 1976; Mittelstaedt, 1991; Mason et al., 2011). The meridional shift of the Trade winds causes seasonal upwelling variability in the north and south extreme regions of the CCUS, while in the central region upwelling is relatively continuous all year round (Wooser et al., 1976; Aristegui et al., 2004). The upwelled relatively cold and nutrient-rich coastal waters mostly flow offshore in filaments rooted at specific locations along the coast (Demarcq, 1998; Meunier et al., 2012); eddies transport nutrients from the upwelling region westward in the oligotrophic North Atlantic (Lumpkin and Garzoli, 2005; Alpers et al., 2013).

The large scale circulation in the CCUS (Figure 1a) is dominated by the eastern branch of the north Atlantic subtropical gyre composed of the Azores (AzC), Portugal (PC) and Canary Currents (CC) (Barton, 1998; Lathuiliére, 2008). South of 20°N the CC flows southwestward and joins the North Equatorial Current (NEC) (Mittelstaedt, 1991), which forms the southern part of the subtropical gyre. Between 5°N and 10°N the dominant feature is the eastward flow known as the North Equatorial Counter Current (NECC) (Lázaro et al., 2005). Near the African coast part of the NECC turns northward, forming the Mauritania Current (MC). The MC shows a strong seasonal variability associated with the NECC and the wind field intensities. In winter and early spring the NECC is weaker, the wind is favourable to coastal upwelling between 14°N and 20°N and the MC is located south of 15°N. While in summer and early autumn the strengthening of the NECC and the relaxation of the northeasterly Trade winds favour the northward migration of the MC that can reach as far as 20°N (Lázaro et al., 2005). Southeast of the Cape Verde Archipelago there is a large scale cyclonic circulation associated with the NEC, the NECC and the MC and called Guinea Dome (GD). The core of this structure is located near 9°N, 25°W in the summer months, at 10.5°N, 22°W in the winter months (Stramma et al., 2005) and near 12°N, 26°W in fall (Doi et al., 2009).

The southern portion of the CCUS, defined in this paper as the region between 12°N and 22°N (see Figure 1 for geographical references), is characterised by upwelling events with a marked seasonal periodicity and with maximal intensity in winter (Wooster et al., 1976; Aristegui et al., 2004, Ndoye et al., 2014). In the framework of the COCES (Coastal Ocean Circulation Experiment off Senegal) and COCES II projects, this region was deeply investigated with the aim of describing its peculiar upwelling features. The COCES and COCES II projects led to the deployment of more than 100 drifters off the Senegal coast in the period 2009-2013. The tracks of these drifters were used in concert with satellite data – sea surface temperature (SST) and chlorophyll-a concentration (Chl-a)

– and other ancillary data (upwelling index and re-analysis wind) to improve our knowledge of the NW Africa upwelling system with particular focus on the Senegal and Mauritania coastal areas. The study area was divided in five geographical sectors and the different upwelling features of these sectors, the relative implications for the ecosystem as well as the main circulation features related with the transport of cold waters, were analysed and compared. Details about the data used in this study are illustrated in Section 2, a description of the intra- and inter-annual variability of the upwelling seasons 2009-2013 are presented in Section 3. Sections 4 and 5 include a discussion of the results and main conclusions.

2. Data and methods

2.1. Satellite data

Moderate Resolution Imaging Spectroradiometer (MODIS) 8-day composite maps of SST and Chl-a (http://oceancolor.gsfc.nasa.gov/DOCS/), focused on the region 8°-22°N, 12°-22°W and gridded with a spatial resolution of ~ 5 km, were used to define the main characteristic of the upwelling season along the Senegal and Mauritania coasts in the period 2009-2013. The spatial (latitudinal) and temporal extensions of the upwelling events were identified using Hovmoller diagrams of the zonally averaged SST over the coastal area extending from the coast to the 2000 m isobath (Figure 1b). This area was divided in five sectors according to the latitudinal evolution of the SST and the geographical characteristic of the region. More specifically, 3 sectors are located around the main Capes and the other 2 in the region between the Capes (see Figure 1b). Time series of the monthly spatially averaged SST obtained in each sector were used to describe the annual and interannual fluctuations related to upwelling processes. The surface cooling from the upwelled water reaching the sea surface is a potential proxy of the upwelling intensity (Benazzouz et al., 2014).

The flow of cold water along the Senegal and Mauritania coasts was qualitatively described superimposing the COCES/COCES II drifter tracks on the normalised SST anomaly maps (see Subsection 2.4 for more details about drifter data). The normalised SST anomaly is obtained by subtracting the mean value of SST from the MODIS composite maps and dividing by the corresponding standard deviation. Representative snapshots of the main upwelling episodes were selected and are showed in Subsection 3.3.

2.2. Upwelling index

Ekman transport data provided by the NOAA Environmental Research Division (Upwelling and Environmental Index Products, http://www.pfeg.noaa.gov) were downloaded for the period 2009-2013. Ekman mass transport is defined as the wind stress divided by the Coriolis parameter; it is resolved into components parallel or normal to the local coastline orientation. Upwelling index from

Ekman transport data (UI_E) can be calculated as the magnitude of the transport component in the direction perpendicular to the shoreline (Gomez-Gesteira et al., 2008) and represents the volume per unit of time of the water being upwelled from the base of the Ekman layer. The monthly-averaged coastal upwelling index UI_E was considered at five points selected along the coast (colored circles in Figure 1b), each one located in a sector (SCV 13.8°N-16.8°W; CV 14.5°N-17.5°W; MA 17°N-16°W; CT 19.4°N-16.6°W; CB 21°N-17°W). Generally, Positive (negative) UI_E values mean upwelling favorable (unfavorable) conditions. In the southern CCUS the monthly-averaged UI_E shows a pronounced seasonality related to the upwelling and non-upwelling conditions, but it is positive everywhere (see Figure 4a) creating the need to define a threshold to identify the upwelling events. The upwelling favorable conditions are established when $UI_E > 150$ $m^3/s/100$ m coastline, corresponding to meridional (upwelling favourable) wind intensities larger than 5 m/s in each sector of Figure 1b.

2.3. Wind data

The time series of wind products in the region of Cape Vert were downloaded from the NOAA website (ERDDAP - NOAA/NCDC Blended Daily 0.25-degree Sea Surface Winds - Data Access Form). These products include globally gridded, high resolution ocean surface vector winds on a global 0.25° grid with a time resolution of 6 h. The wind speeds were generated by blending observations from multiple satellites; the wind directions came from two sources depending on the products: NCEP reanalysis 2 or ECMWF.

2.4. Drifter data and processing

As part of the COCES and COCES II projects, 109 surface drifters were deployed off Senegal between May 2009 and June 2013. Two types of drifters were used: the Surface Velocity Program (SVP) drifter (Sybrandy and Niiler, 1991) and the Coastal Ocean Dynamic Experiment (CODE) drifter (Davis, 1985).

All drifters were tracked by polar-orbiting Argos satellites. The drifter position time series were edited from spike and outliers, then linearly interpolated at regular 2-h intervals using the kriging technique (optimal interpolation; Hansen and Poulain, 1996; Poulain et al., 2004a). The interpolated positions were finally sub-sampled at 6-h intervals. Velocity components were then estimated from centered finite differences of 6-h sub-sampled positions. The entire dataset includes 45232 6-h data points, corresponding to more than 30 drifter - years.

3. Results

Hovmoller diagrams of zonally averaged SST (Figure 2) describe the main characteristics of the upwelling in the southern CCUS (area of averaging depicted in Figure 1b) during the period 2009-

2013. The isotherms of 24°C define the boundary between the cold upwelled and the warm resident waters. The area interested by upwelling is located north of 12°N and the length of the upwelling seasons increases with increasing latitude: they last from January to May in the region south of Cap Vert (SCV; 12-14°N), from December/January to June in the region around Cape Vert (CV; 14-16°N), from December/January to June/July off the southern Mauritania coast (MA; 16°-18°N), from November to July in the area off Cap Timiris (CT; 18-20°N) and from October to July in the region of Cape Blanc (CB; 20-22°N). Cold waters observed south of 12°N are not ascribable to upwelling events, but they are transported southward by surface currents from the adjacent (northern) regions, as described in more detail in Subsection 3.3.

Time series of the monthly data, obtained from different sources (upwelling index, satellite data, wind products) and spatially averaged in the five sectors defined in the previous paragraph (Figures 1b), were compared in order to describe the annual and interannual upwelling variability along the northwest Africa coast (Subsections 3.1 and 3.2, respectively).

The horizontal patterns associated with the upwelling seasons were investigated by means of SST anomaly maps and drifter tracks in Subsection 3.3.

3.1. Annual evolution of the coastal upwelling conditions

The annual evolution of the UI_E, SST and Chl-a, calculated by averaging the monthly data from 2009 to 2013, allows to illustrate the upwelling favorable conditions in the five sectors of Figure 1b. The effect of the wind forcing (Ekman transport) on the ocean water is described in terms of presence of upwelled water (SST) and implications of upwelling for the ecosystem (Chl-a). Surface wind flux and coastal SST are two complementary parameters to quantify the spatial extent and intensity of the upwelling processes, the first one from physical theory and the second one based on direct observations (Benazzouz et al., 2014).

The annual time series of UI_E are exclusively composed by positive values (Figure 3a), therefore the downwelling conditions can be excluded in the entire study area. The Ekman transport shows upwelling favorable conditions (> 150 m^3/s/100 m coastline) from January to June in the southern sectors (defined hereafter as SCV, CV), between January and July in the MA sector and from February to December in the northern sectors (defined hereafter as CT and CB); it achieves its largest values in April, May and June, respectively.

The annual cycle of SST (Figure 3b) roughly follows the seasonal fluctuation outlined by UI_E (Figure 3a). The SST increases gradually from north (CB sector) to south (SCV sector). According to the results of Figure 2, an approximate threshold between the upwelling favorable/unfavorable conditions is defined at 24°C (Figure 3b). The main differences with UI_E are observed during November, December and January in the northern sectors, where the presence of cold upwelled

waters are not supported by increments of the Ekman offshore transport (compare Figures 3a and 3b).

In the southern and MA sectors the Chl-a (Figure 3c) increases gradually between October and May and drops in late spring, following the annual evolution of UI_E and SST. More precisely Chl-a decreases in May in the SCV sector, in June in the CV sector and in July in the MA sector, exhibiting a northward propagation in agreement with Lathuiliere et al. (2008). Highest mean values, as large as 1.2 mg/m^3, are observed south of Cape Vert in April (SCV sector in Figure 3c); lowest mean values (lower than 0.2 mg/m^3) are detected in June, July and October in the MA sector. In the northern sectors the Chl-a (Figure 3d) show an opposite behaviour: the Chl-a gradually increases/decreases between January and June in the CT/CB sectors, respectively; in July it drops in the CT sector and rises in the CB sector.

3.2. Interannual variability of the upwelling conditions

Time series of the monthly spatially averaged UI_E (Figure 4a) and SST (Figure 4b) summarize the main inter-annual characteristics of the upwelling seasons in the period 2009-2013. The Ekman transport is stronger in 2009 with respect to the following years (Figure 4a) and leads to SST colder than 18°C also in the southern sectors (Figures 2 and 4b). The fluctuations of UI_E (Figure 4a) shows a phase shift between the southern sectors, where the maximum Ekman transport occurs between March and May, and the northern sectors, where the maximum occurs in June-July. The upwelling favourable Ekman transport is generally larger in the southern and MA sectors, where it is in phase with the occurrence of the SST minimal values (Figure 4b); indeed, the negative correlation between these two variables is largest at zero time lag (the correlation coefficient is -0.89 in the southern sectors and -0.66 in the MA sector). The northern sectors display a time lag between the atmospheric forcing and the ocean response, with largest negative correlation (~ -0.6) correspondent with a lag of 7-9 months.

The southern and MA sectors show the typical increase of the Chl-a during the months of upwelling (values generally larger than 0.5 mg/m^3 between February and May), more accentuated in the SVC sector during the upwelling seasons 2011 (Figure 4c) and in the CV sector during 2010 and 2012. In the CB sector (Figure 4d) higher values of Chl-a are observed in summer (August-September) and early fall (October-November). The CT sector has a not clear trend with maxima values in fall during 2009-2010, in winter in 2011 and 2012 and in spring in 2013 (Figure 4d). The higher Chl-a concentration in the southern sectors, compared to the northern region, was already observed in Lathuiliere et al. (2008) over the period 2000-2004, and was ascribed to the nutrient richness of subsurface water in this area caused by a shallow nutricline. Sometime, similar increments of the UI_E in different sectors do not correspond to similar responses of the ecosystem, e.g. a similar

206 increment of offshore Ekman transport in the SCV and CV sectors in March-April 2011 (Figure 4a)
207 correspond with the maximum of Chl-a in the SCV time series but not in the CV time series (Figure
208 4c). The strengthening/weakening of the offshore Ekman transport is indeed not sufficient to
209 explain the Chl-a increase/decrease but, as suggested in Lathuiliere et al. (2008), another process
210 involved is the pre-existent nutrient availability in the surface layer. During winter the nitrate
211 surface concentration is quite high, indicating that the limitation by nutrient is weak (see Figure 3d
212 of Lathuiliere et al., 2008 and Figure 7 of Deme-Gningue, 1998). Therefore, a new input of
213 nutrients by an upwelling-favourable wind event could not trigger an immediate and robust
214 response of the ecosystem, as in winter/spring 2011 in the CV sector.

215 *3.3. Upwelling seasons during 2009-2013*

216 In this subsection the COCES/COCES II drifter tracks, superimposed with the normalised SST
217 anomaly maps, are used to describe the main circulation features related with the transport of cold
218 waters during the upwelling seasons. Each figure contain four panels composed by consecutive 8-
219 days SST anomaly maps (Figures 5-8), specifically selected to emphasize the flow of cold water
220 offshore and alongshore, overlapped with concurrent drifter trajectories (white lines).
221 In winter 2010 the SST anomaly maps define the occurrence of cold water filaments generated
222 along the coast in correspondence to the capes (Cap Vert, Cap Timiris and Cap Blanc) and off the
223 southern Mauritania coast at 16°-19°N (Figures 5); they extend offshore for ~100-150 km with a
224 mean temperature of ~18-20°C. Drifters deployed in the Cap Vert filament (Figure 5a) record
225 speeds of 30-40 cm/s and are mainly transported south-westward (Figure 5b and 5c). Cold water,
226 originated from upwelling events south of Cape Vert, are transported southward by surface currents
227 producing a tongue of cold water on the Gambia continental shelf (Figures 5a and 5b). Drifters
228 deployed in this region are transported southward (Figures 5a, 5b and 5c) with speed of 20-30 cm/s.
229 In spring 2011, two drifters deployed north of Cap Vert move northward parallel to the coast
230 (Figures 6a and 6b) with speeds larger than 40 cm/s, following the pathway of the MC, then turn
231 westward transported by the filament of cold water located at ~ 18°N (Figure 6c and 6d; speeds of
232 20-30 cm/s). The third drifter deployed north of Cap Vert is transported south-westward (Figures
233 6b, 6c and 6d) with speeds larger than 30 cm/s. Cold water upwelling filaments are well defined in
234 the second half of April (Figures 6c and 6d), especially the Mauritania filament that extend offshore
235 for more than 200 km. The cold water south of Cape Vert is mostly advected southward; is
236 southernmost extension occurs in late spring (Figure 6d).
237 In winter-spring 2012, drifters deployed off Cape Vert move northward along the coast with speeds
238 of 30 cm/s; Figures 7a and 7b) and turn westward, following the upwelling filaments off the
239 Mauritania coast (between 16.5°N and 18°N; Figures 7b and 7d), or southward (Figure 7d) or are

captured by mesoscale features (diameters of ~ 50 km) off the Senegal and Mauritania coasts (Figures 7c and 7d). Drifters deployed south of Cape Vert (Figure 7a) recirculate in the region of deployment (Figures 7b and 7c), then are transported southward (Figure 7d).

In winter-spring 2013, drifter deployed on the Senegal continental shelf south of Cape Vert moves northward with speeds of 30-40 cm/s, showing the pathway of MC (Figures 8a and 8b). Between 16°N and 17°N drifters turn westward (Figure 8c) and are transported south-westward (Figure 8d) with speed of 20-30 cm/s.

In summary, drifter tracks show the main meridional currents along the coast and zonal currents offshore. North of Cap Vert the coastal circulation (< 100 km from the coast) is directed poleward, whereas the main offshore westward currents are located in the region of the Mauritania filament (between 16.5°N and 18°N). South of Cap Vert the coastal currents are directed equatorward and the offshore circulation is oriented south-westward.

4. Summary and Discussion

Over the last years, several works were carried out in order to describe and quantify the upwelling events in the CCUS. Nevertheless, most of these studies were mainly focused on the northern (Alvarez et al., 2011) or southern areas (Ndoye et al., 2014) of the CCUS and generally they considered the Senegal and Mauritania region as an unique system characterised by high seasonality (Benazzouz et al., 2014) and modulated by the seasonal translation of the Trade winds along the western African coast (Demarcq and Faure, 2000). This study proposes a deepened analysis of the Senegal and Mauritania coastal area in the period 2009-2013 and a comparative investigation of the different geographical sectors that compose this region. Upwelling conditions were analysed in terms of Ekman transport upwelling index and of time series of the satellite SST, Chl-a and wind products. The horizontal structure of the upwelling processes was described using maps of SST anomalies and drifter tracks.

The area interested by upwelling is located north of 12°N and the length of the upwelling seasons increases from south to north (Figure 2). The mean annual evolution of UI_E (Figure 3a) shows that the periods characterized by more upwelling favorable conditions correspond to December-June in the southern sectors (SCV, CV) and to February-October in the northern sectors (CT and CB) with higher values (as large as 600 m^3 s^{-1}/100 m of coastline) in April/May and June, respectively. The fluctuation of wind forcing plays a direct effect on the ocean water and on the ecosystem in the southern and in the MA sectors (Figures 3b, 3c and 3d), whereas the northern sectors are characterized by cold upwelled water also in the months with low values of UI_E.

In the southern sectors the interannual evolution UI_E and SST are in phase (higher values of UI_E correspond with lower SST; Figures 4a and 4b), which means that the upwelling is tightly linked to the seasonality of the trade winds, without time lag, in agreement with the results of Benazzouz et al. (2014) in the same area. The northern sectors show a fluctuation that is out-of-phase with respect to the southern sectors (Figure 4a) with a lag between the atmospheric forcing and the ocean response of about 7-9 months. Cropper et al. (2014) have observed an increase of the summer downwelling favorable conditions south of 19°N in the period 1981-2012; this trend is confirmed by the results of the present study which show a weakening of the Ekman offshore transport during 2009-2013.

The implications of the upwelling for the ecosystem have been characterised using the time series of the Chl-a concentrations (Figures 4c and 4d). In the southern sectors Chl-a shows a high variability related with the occurrence of upwelling and non-upwelling seasons; the highest concentration values are observed in the SCV sector during the upwelling seasons 2011 and in the CV sector during 2010 and 2012 (Figure 4c). In the northern sectors the Chl-a show an high interannual variability not affected by the upwelling seasonal fluctuation (Figure 4d). The two distinct behaviours of the Chl-a along the Senegal and Mauritania coasts were already detected from Lathuliere et al. (2008). These authors have distinguished the region between 10°N and 19°N, characterised by a large seasonal cycle and by a significant correlation with the wind stress, from the region between 19°N and 24°N, characterised by a small amplitude of the seasonal cycle and no significant correlation with the wind stress.

The maps of SST anomalies allow to discriminate the cold water filaments associated with the upwelling events along the Senegal and Mauritania coast. These recurrent upwelling filaments (SST lower than 18°C) are generally located north of Cap Vert, off the southern Mauritania coast, south of Cap Timiris and in the Cap Blanc area (Figures 5-8). The filaments persist for a few weeks, and they subsequently mix with the surrounding waters. The filaments formation off the capes is generally associated with the topographic and coastline morphology of the region. This dynamical process is common to the other upwelling regions as explained by Dale and Barth (2001) with important implication for the transport of shelf water to the deep ocean (Barth et al., 2000). The wind vorticity reinforces the upwelling near the capes via Ekman pumping, as seen along the California coast (Paduan et al., 1990) or in the Adriatic (Poulain et al., 2004b). Tongues of cold water can be observed on the Senegal continental shelf south of Cap Vert in the region between 10°N and 15°N; the southernmost extention of these tongues occurs in spring in good agreement with Roy (1998), Demarcq (1998) and Demarcq and Faure (2000).

Drifter tracks allow to add some details about the flow of cold water offshore and alongshore. In particular they describe: (1) the westward zonal transport of waters from the coast toward the Cape Verde Archipelago in correspondence to the Mauritania coast (Figures 6c, 6d, 7d, 8d) (2) the south-westward transport of the coastal water in the region of Cap Vert and south of Cape Vert (Figures 5, 7c, 7d); (3) the northward MC off the Senegal and Mauritania coasts (Figures 6a, 7a, 7b).

5. Conclusions

This work contributes to improve the knowledge on the variability of the Senegal and Mauritania upwelling system over seasonal and interseasonal timescales. Previous works have already emphasized strong latitudinal variations along the coast, in particular between the northern and the southern ends of CCUS, but the geographical limits of the sectors with similar characteristics were not precisely defined and the Senegal and Mauritania coasts were frequently classified as an unique system with homogeneous features. The results of this work show a gradual increase of the length of the upwelling season with the latitude and lead to define two regions along the Senegal and Mauritania coasts with fairly different behaviour: a northern sector, that includes the region off Cap Blanc and Cap Timiris (north of 18°N) and a southern sector, located south of 16°N.

In the northern sector the cold upwelled waters are detected between October and July and their presence appear not influenced by the annual fluctuation of Ekman transport, that shows upwelling favourable conditions between February and October. The maximum annual value of the Chl-a is of 0.8-0.9 mg/m^3. The southern sector exhibits a strong seasonal variations and the core of the upwelling season occurs from December to June. The fluctuation of wind forcing plays a direct effect on the ocean water and on the ecosystem response, without time lag. The Chl-a increases gradually from October to May and drops in late spring.

The main limitation of this approach is that 5-years time series are too short to clearly define a trend in the upwelling and to correlate the interannual variation of the variables with large-scale and local climatic patterns. This issue can constitute a starting point for a future analysis, which will take into account longer time series of satellite and in-situ data and their relation with global atmospheric teleconnection patterns.

Acknowledgments

The authors would like to thank all the people who helped with drifter deployments and recoveries. We also thank A. Bussani for the processing and on-line visualization of drifter data. This work was supported by the U.S. Office of Naval Research under contracts N000140811038 and N000141110480.

References

Alpers W., Brandt P., Lazar A., Dagorne, D., Sow B., Faye S., Hansen M.W., Rubino, A. Poulain, P.-M. and Brehmer, P.; 2013: A small-scale oceanic eddy off the coast of West Africa studied by multi-sensor satellite and surface drifter data. Remote Sens. Environ., 129, 132-143.

Alvarez I., Gomez-Gesteira M., de Castro M., Lorenza M.N., Crespo A.J.C. and Dias J.M.; 2011: Comparative analysis of uwelling influence between the western and northern coast of the Iberia Peninsula. Cont. Shelf Res., 31, 388-399.

Aristegui J., Alvarez-Salgado X.A., Barton E.D., Figueiras F.G., Hernandez-Leon S., Roy, C. and Santos A.M.P.; 2004: Oceanography and fisheries of the Canary Current/Iberia region of the eastern North Atlantic. The Sea, 14.

Aristegui J., Barton E.D., Alvarez-Salgado X.A., Santos M., Figueiras F.G., Kifani S., Hernandez-Leon S., Mason E. and Demarcq H.; 2009: Sub-regional ecosystem variability in the Canary Current upwelling. Prog. Oceanogr., 83, 33-48.

Barth J.A., Pierce S.D. and Smith R.L.; 2000: A separating coastal upwelling jet at Cape Blanco, Oregon, and its connection to the California Current system. Deep-Sea Res. Pt. II, 47, 783-810.

Barton E.D.; 1998: Eastern boundary of the North Atlantic: Northwest Africa and Iberia. In A.R. Robinson, & K.H. Brink (Eds.), The sea, the global coastal ocean: regional studies and syntheses, New York, Vol.11, pp 633-657.

Benazzouz A., Mordane S., Orbi A., Chagdali M., Hilmi K., Atillah A., Pelegrí, J.L. and Demarcq H.; 2014: An improved coastal upwelling index from sea surface temperature using satellite-based approach – The case of the Canary Current upwelling system, Cont. Shelf Res., 81, 38-54.

Copper E.T., Hanna E. and Bigg G.R.; 2014: Spatial and temporal seasonal trends in coastal upwelling off Northwest Africa, 1981-2012. Deep Sea Res. I, 86, 94-111.

Dale A.C. and Barth J.A.; 2001: The hydraulics of an evolving upwelling jet flowing around a cape. J. Phys. Oceanogr., 31, 226-243.

Davis R.E.; 1985: Drifter observations of coastal currents during CODE. The method and descriptive view, J. Geophys. Res., 90, 4741-4755.

Demarcq H.; 1998: Spatial and temporal dynamics of the upwelling off Senegal and Mauritania: local change and trend. Global versus local changes in upwelling systems, 149-166, ORTSOM ed., Paris.

Demarcq H. and Faure V.; 2000: Coastal upwelling and associated retention indices derived from satellite SST. Application to Octopus vulgaris recruitment. Oceanol. Acta, 23(4), 391-408.

Deme-Gningue I.; 1998: Trends and variability of environmental time series along the Denegalese coast. Global versus local changes in upwelling systems, 179-192. ORSTOM ed., Paris.

Doi T., Tozuka T. and Yamagata T.; 2009: Interannual variability of the Guinea Dome and its possible link with the Atlantic Meridional Mode. Clim. Dyn., 33, 985-998. doi: 10.1007/s00382-009-0574-z.

Gomez-Gesteira M., deCastro M., Alvarez I., Gomez-Gesteira J.L.; 2008: Coastal sea surface temperature warming trend along the continental part of the Atlantic Arc (1985–2005). J. Geophys. Res., 113, C04010. doi:10.1029/2007JC004315.

Hansen D.V. and Poulain P.-M.; 1996: Processing of WOCE/TOGA drifter data. J. Atmos. Ocean. Tech., 13, 900-909.

Lathuiliére C., Echevin V. and Lévy M.; 2008: Seasonal and interseasonal surface chlorophyll-a variability along the northwest African coast. J. Geophys. Res., 113, C05007. doi 10.1029/2007JC004433.

Lázaro C., Fernandes M.J., Santos A.M.P. and Oliveira P.; 2005: Seasonal and interannual variability of surface circulation in the Cape Verde region from 8 years of merged T/P and ERS-2 altimeter data. Remote Sens. Environ., 98, 45-62.

Lumpkin R. and Garzoli S.L.; 2005. Near-surface circulation in the Tropical Atlantic Ocean. Deep-Sea Res. I, 52, 495-518.

Mason E., Colas F., Molemaker J., Shchepetkin F., Troupin C., McWilliams J.C. and Sangrà P.; 2011: Seasonal variability of the Canary Current: A numerical study. J. Geophys. Res., 116, C06001.

Marchesiello P., Herbette S., Nykjaer L. and Roy C.; 2004: Eddy-driven dispersion processes in the Canary Current upwelling system: comparison with California System. GLOBEC International newsletter, 10(1).

Meunier T., Barton E.D., Barreiro B. and Torres R.; 2012: Upwellng filaments off Cap Blanc: interaction of the NW African upwelling current and Cape Verde frontal zone eddy field?. J. Geophys. Res. 117, C08031. doi: 10.1029/2012JC007905.

Mittelstaedt E.; 1991: The ocean boundary along the northwest African coast: circulation and oceanography properties at the sea surface. Prog. Oceanogr., 26. 307-355.

Ndoye S., Capet X., Estrade P., Sow B., Dagorne D. and Lazar, A.; 2014: SST patterns and dynamics of the Southern Senegal-Gambia upwelling center. Accepted by J. Geophys. Res. Oceans.

Paduan J.D. and Niiler P.P.; 1990: A Lagrangian description of motion in Northern California coastal transition filaments. J. Geophys. Res., 95, C10, 18095-18109. doi: 10.1029/JC095iC10p18095.

Poulain P.-M., Barbanti R., Cecco R., Fayes C., Mauri E., Ursella L. and Zanasca, P.; 2004a: Mediterranean surface drifter database: 2 June 1986 to 11 November 1999. Rel. 75/2004/OGA/31, OGS, Trieste, Italy (CDRom).

Poulain, P.-M., Mauri, E., Ursella L., 2004b. Unusual upwelling event and current reversal off the Italian Adriatic coast in summer 2003. Geophys. Res. Lett., 31, L05303, doi:10.1029/2003GL019121.

Roy C.; 1998: An upwelling-induced retention area off Senegal: a mechanism to link upwelling and retention processes. S. Afr. J. Marine Sci., 19, 89-98.

Santos A.M.P., Kazmin A.S. and Peliz A.; 2005: Decadal changes in the Canary upwelling system as revealed by satellite observations: their impact on productivity. J. Marine Res., 63, 359-379.

Stramma L., Huttl S. and Schafstall J.; 2005: Water masses and currents in the upper tropical northeast Atlantic off northwest Africa. J. Geopys. Res., 110,C12006. doi:10.1029/2005JC002939.

Sybrandy A. L. and Niiler P.P.; 1991: WOCE/TOGA Lagrangian drifter construction manual. SIO Ref. 91/6, WOCE REP. 63, Scripps Institution of Oceanography, La Jolla, California, 58p.

Wooster W.S., Bakun A. and Mclain D.R.; 1976: Seasonal Upwelling Cycle Along Eastern Boundary of North-Atlantic. J. Mar. Res., 34, 131-141.

Figure captions

Figure 1. (a) Geography, bathymetry and main surface current systems off the Northwest Africa coast in the region surrounding the Cape Verde Archipelago. The 1000 m and 2000 m isobaths are shown with light grey lines. (b) Coastal area, enclosed between the coast and the 2000 m isobath, used to estimate the Hovmoller diagrams of Figure 2; colors point out the sectors used to compute the time series of Figures 3 and 4. The acronyms are explained in the text.

Figure 2. Hovmoller diagrams of MODIS 8-day SST averaged zonally over the coastal area depicted in Figure 1b for the years 2009-2013. Black dotted rectangles point out the locations of the sectors defined in Figure 1b.

Figure 3. Annual cycle of the upwelling index UI_E, calculated from Ekman transport (a), SST (b), and Chlorophyll-a concentration (c, d) spatially averaged over the sectors depicted Figure 1b, during the period 2009-2013.

Figure 4. Interannual cycle of the upwelling index UI_E, calculated from Ekman transport (a), SST (b), and Chlorophyll-a concentration (c, d) spatially averaged over the sectors depicted Figure 1b, during the period 2009-2013.

Figure 5. Normalised SST anomaly maps, derived from MODIS 8-day composite maps of SST, selected during the upwelling season 2010 with surface drifter tracks superimposed (white lines). MODIS maps are centred on 17 Feb 2010 (a), 25 Feb 2010 (b), 5 Mar 2010 (c), 13 Mar 2010 (d). Drifter ending points are shown with black circles. Mean values of SST and the relative standard deviation are reported in each panel.

Figure 6. Normalised SST anomaly maps, derived from MODIS 8-day composite maps of SST, selected during the upwelling season 2011 with surface drifter tracks superimposed (white lines). MODIS maps are centred on 6 Apr 2011 (a), 14 April 2011 (b), 22 April 2011 (c), 30 April 2011 (d). Drifter ending points are shown with black circles. Mean values of SST and the relative standard deviation are reported in each panel.

Figure 7. Normalised SST anomaly maps, derived from MODIS 8-day composite maps of SST, selected during the upwelling season 2012 with surface drifter tracks superimposed (white lines). MODIS maps are centred on 12 Mar 2012 (a), 20 Mar 2012 (b), 28 Mar 2012 (c), 5 Apr 2012 (d). Drifter ending points are shown with black circles. Mean values of SST and the relative standard deviation are reported in each panel.

Figure 8. Normalised SST anomaly maps, derived from MODIS 8-day composite maps of SST, selected during the upwelling season 2013 with surface drifter tracks superimposed (white lines). MODIS maps are centred on 13 Mar 2013 (a), 21 Mar 2013 (b), 29 Mar 2013 (c), 6 Apr 2013 (d). Drifter ending points are shown with black circles. Mean values of SST and the relative standard deviation are reported in each panel.

456 Figure 1
457

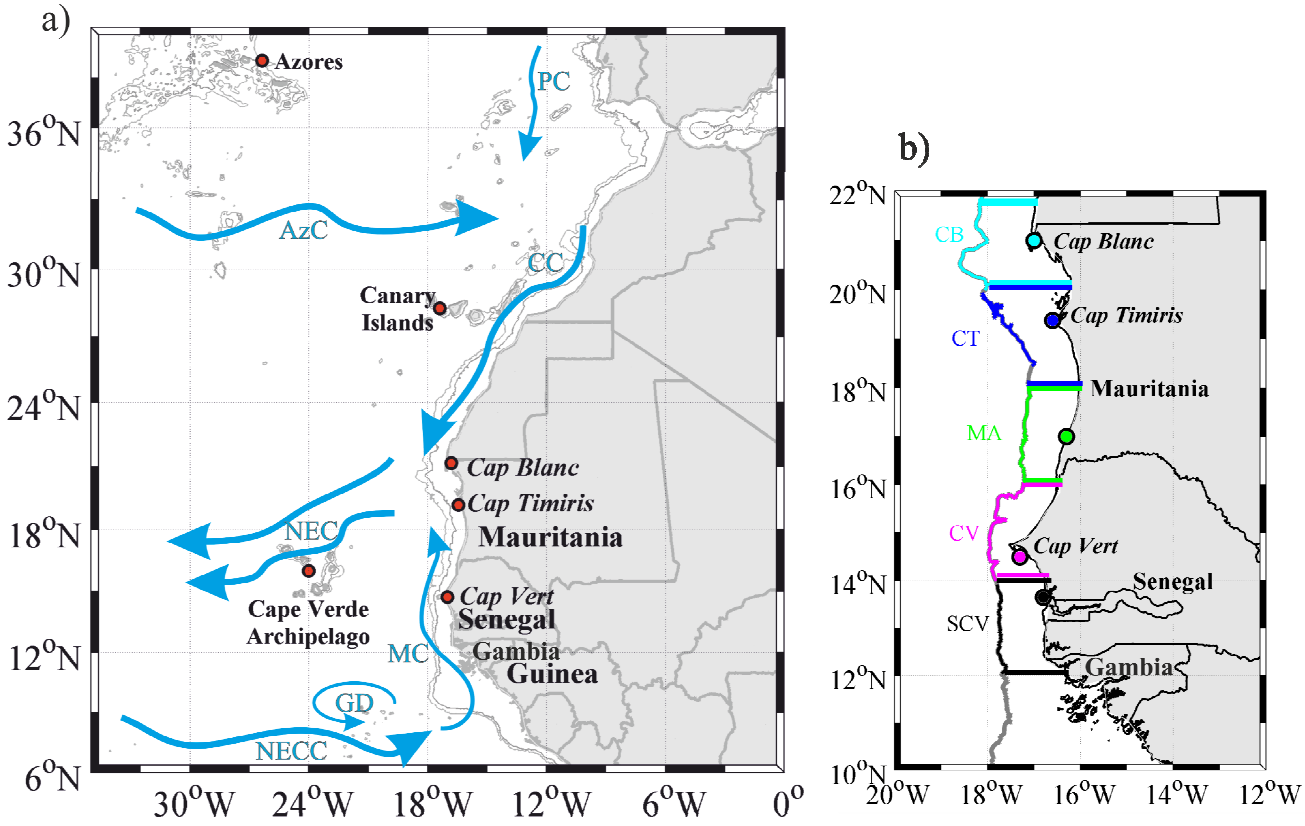

458
459
460
461

462 Figure 2
463

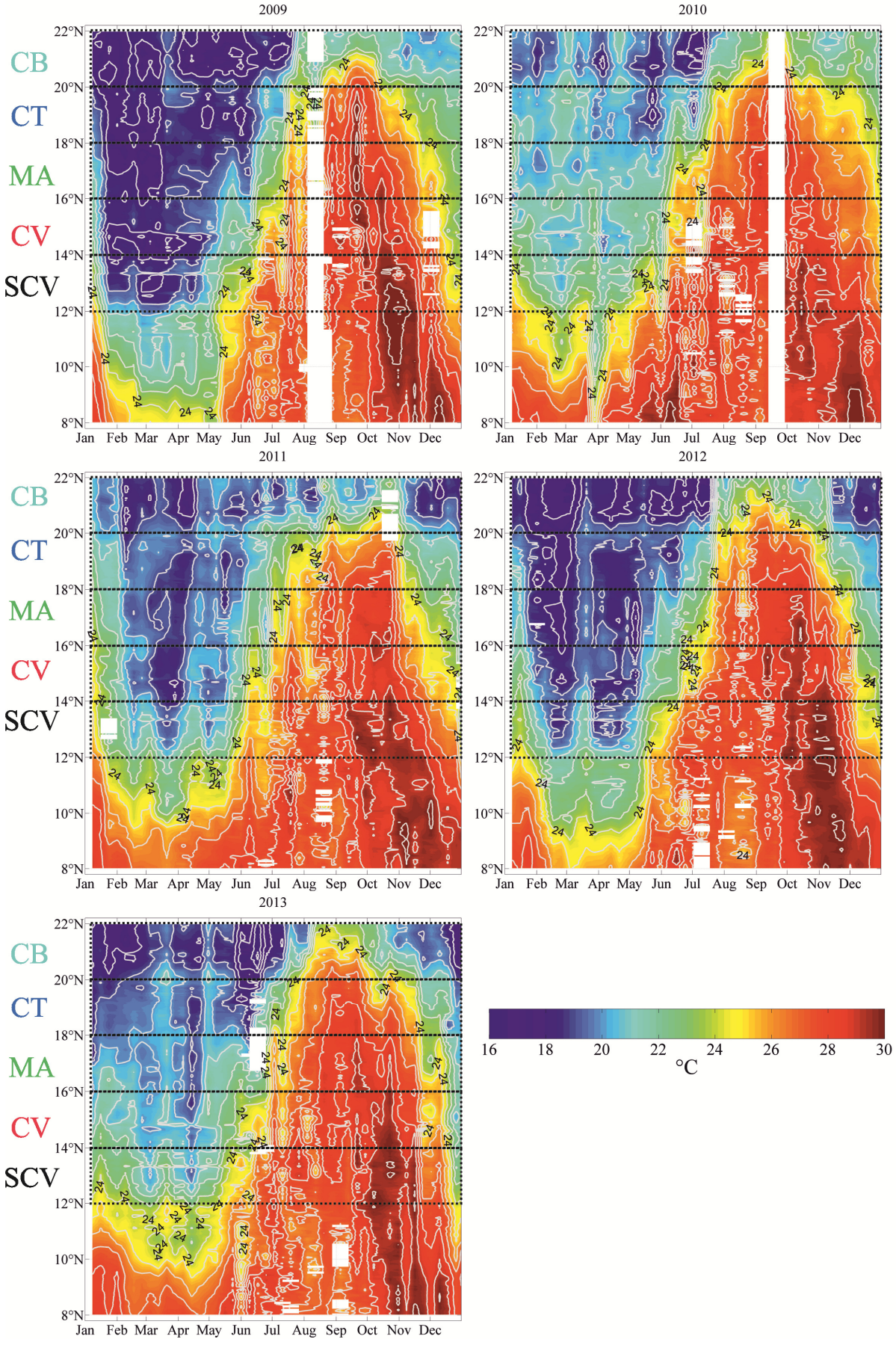

464

Figure 3

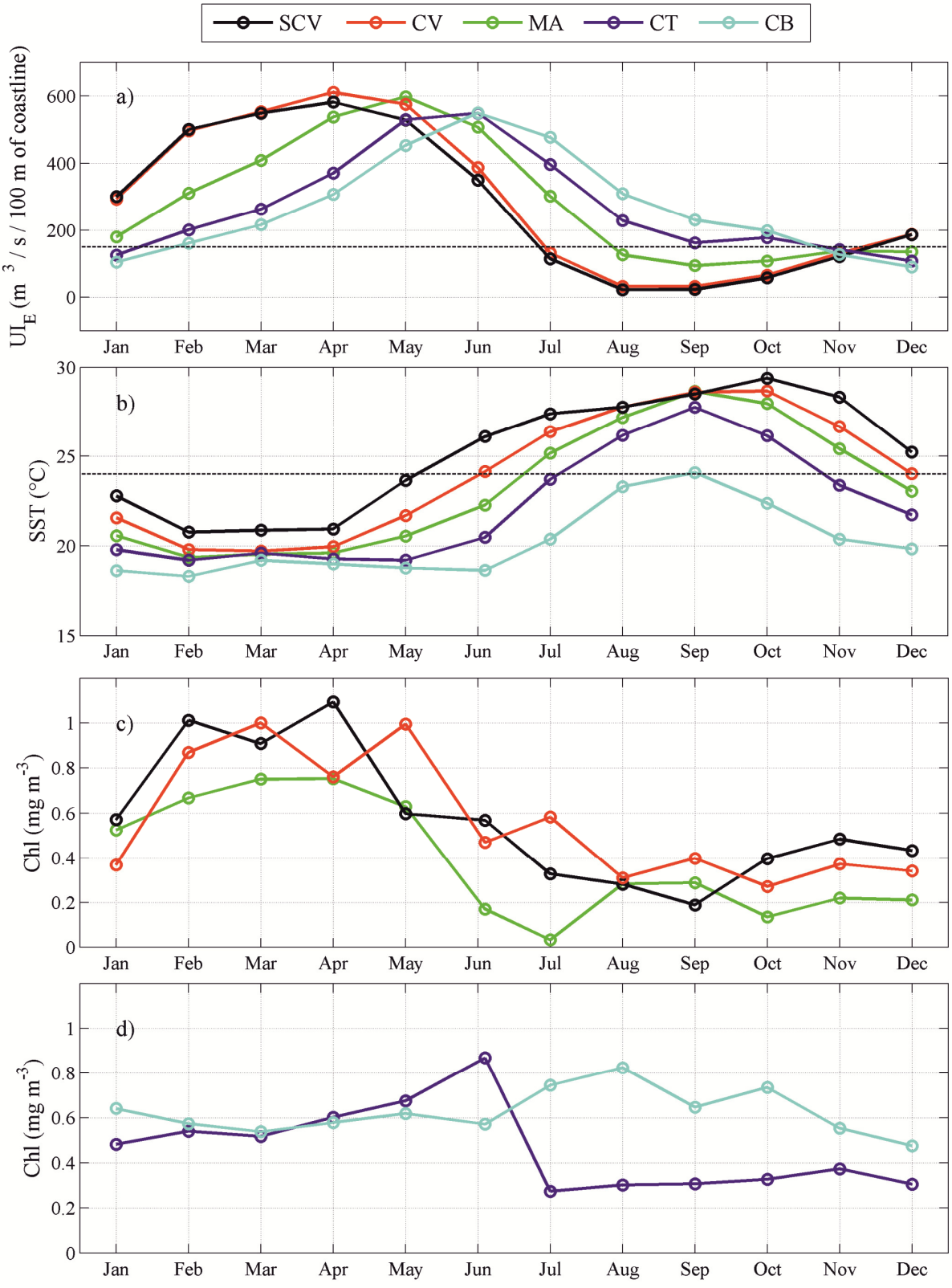
SCV
CV
MA
CT
CB
a)
b)
c)
d)
UIE (m3 / s / 100 m of coastline)
SST (°C)
Chl (mg m-3)
Chl (mg m-3)
Jan
Feb
Mar
Apr
May
Jun
Jul
Aug
Sep
Oct
Nov
Dec

468 Figure 4
469

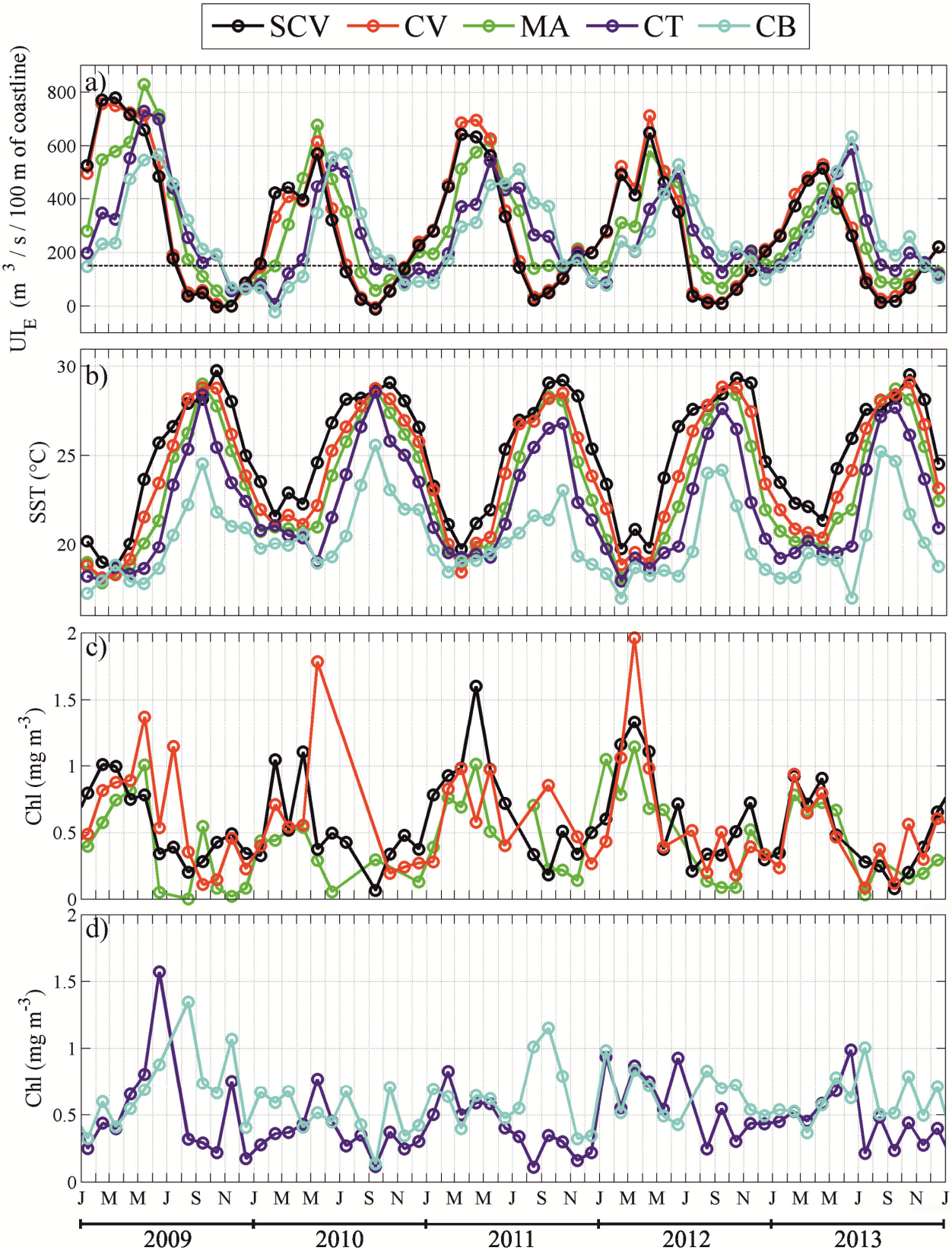

470
471

Figure 5

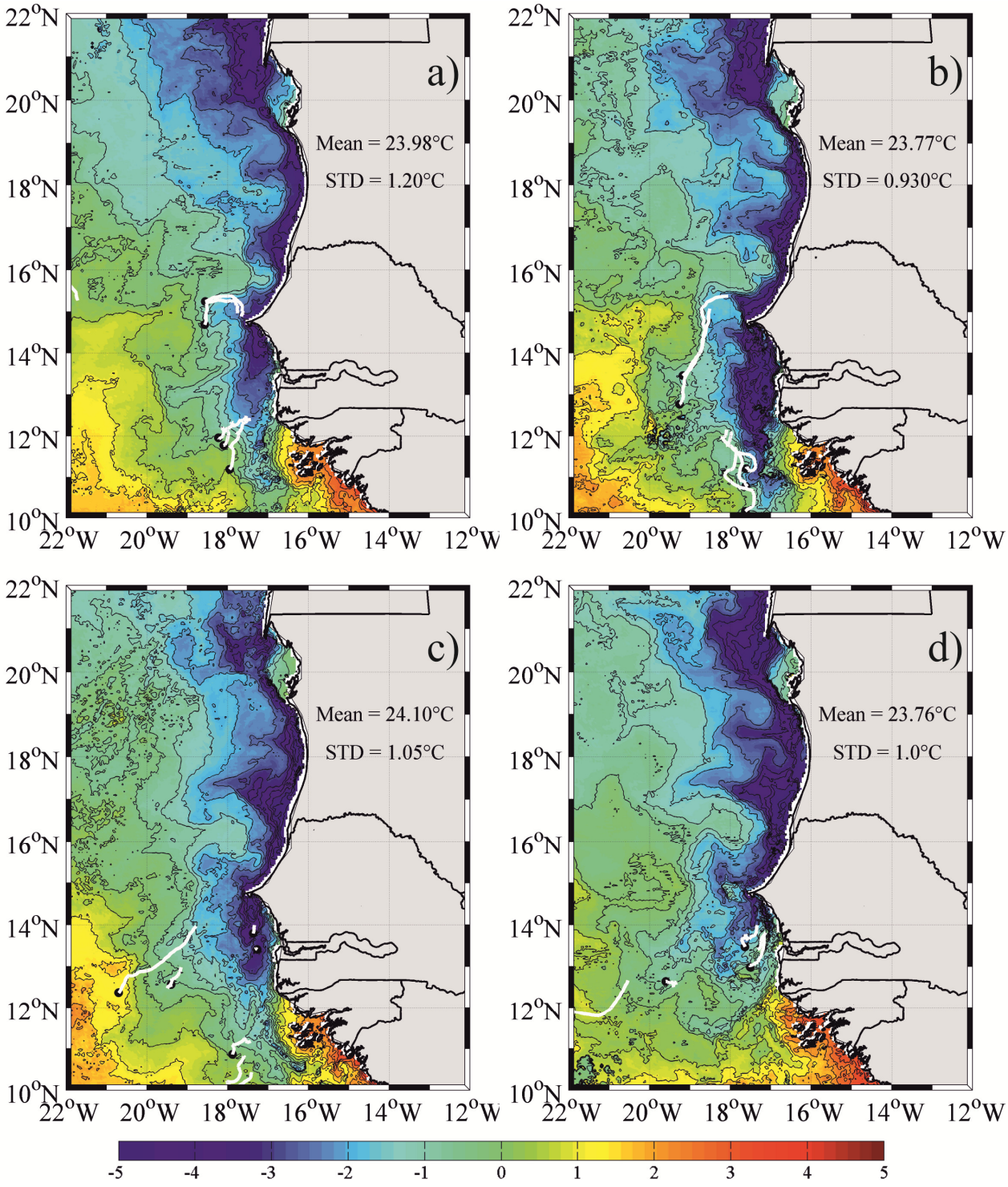
a)
Mean = 23.98°C
STD = 1.20°C
b)
Mean = 23.77°C
STD = 0.930°C
c)
Mean = 24.10°C
STD = 1.05°C
d)
Mean = 23.76°C
STD = 1.0°C
22°N
20°N
18°N
16°N
14°N
12°N
10°N
22°W
20°W
18°W
16°W
14°W
12°W
-5
-4
-3
-2
-1
0
1
2
3
4
5

476 Figure 6
477

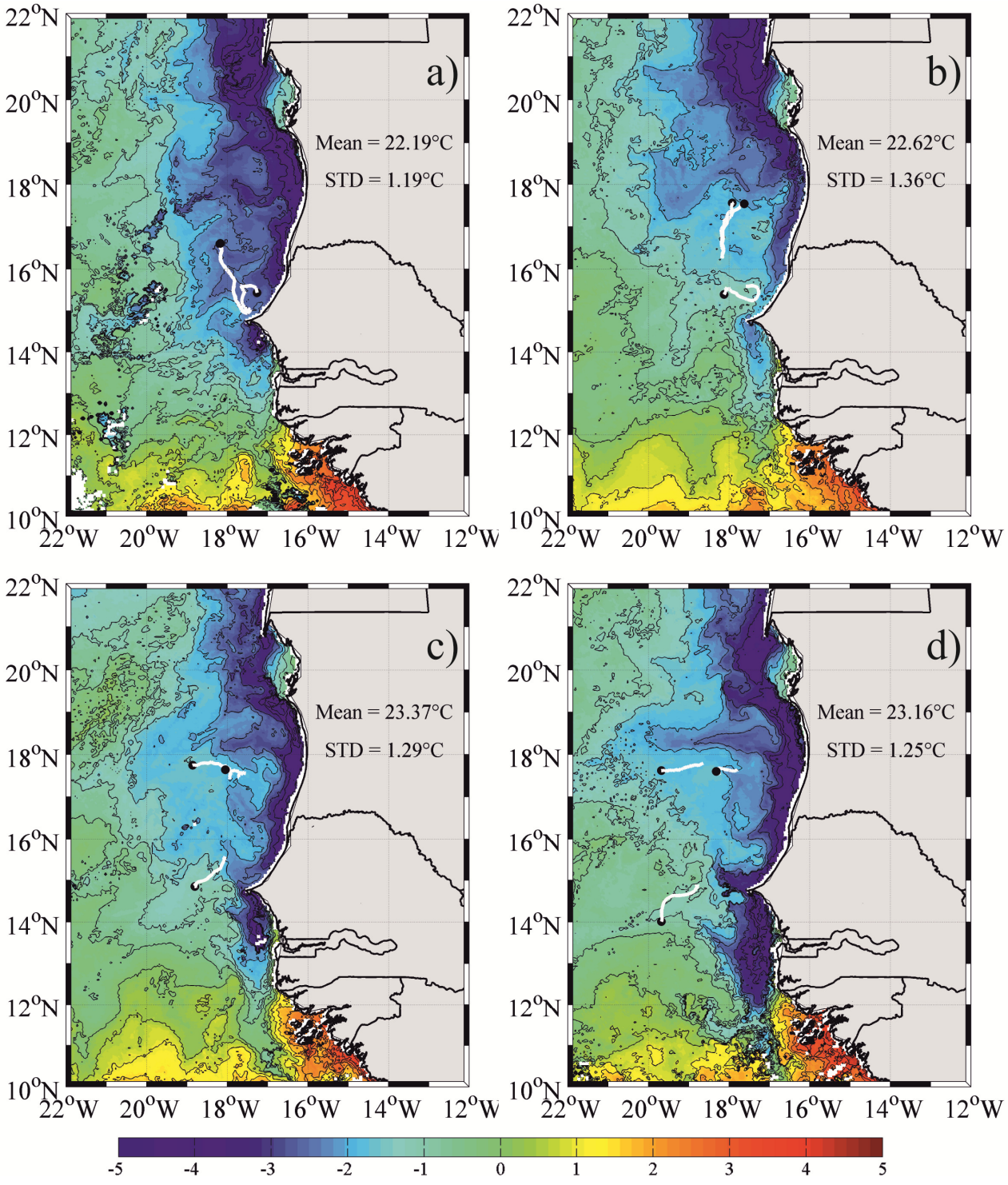

478
479

480 Figure 7
481

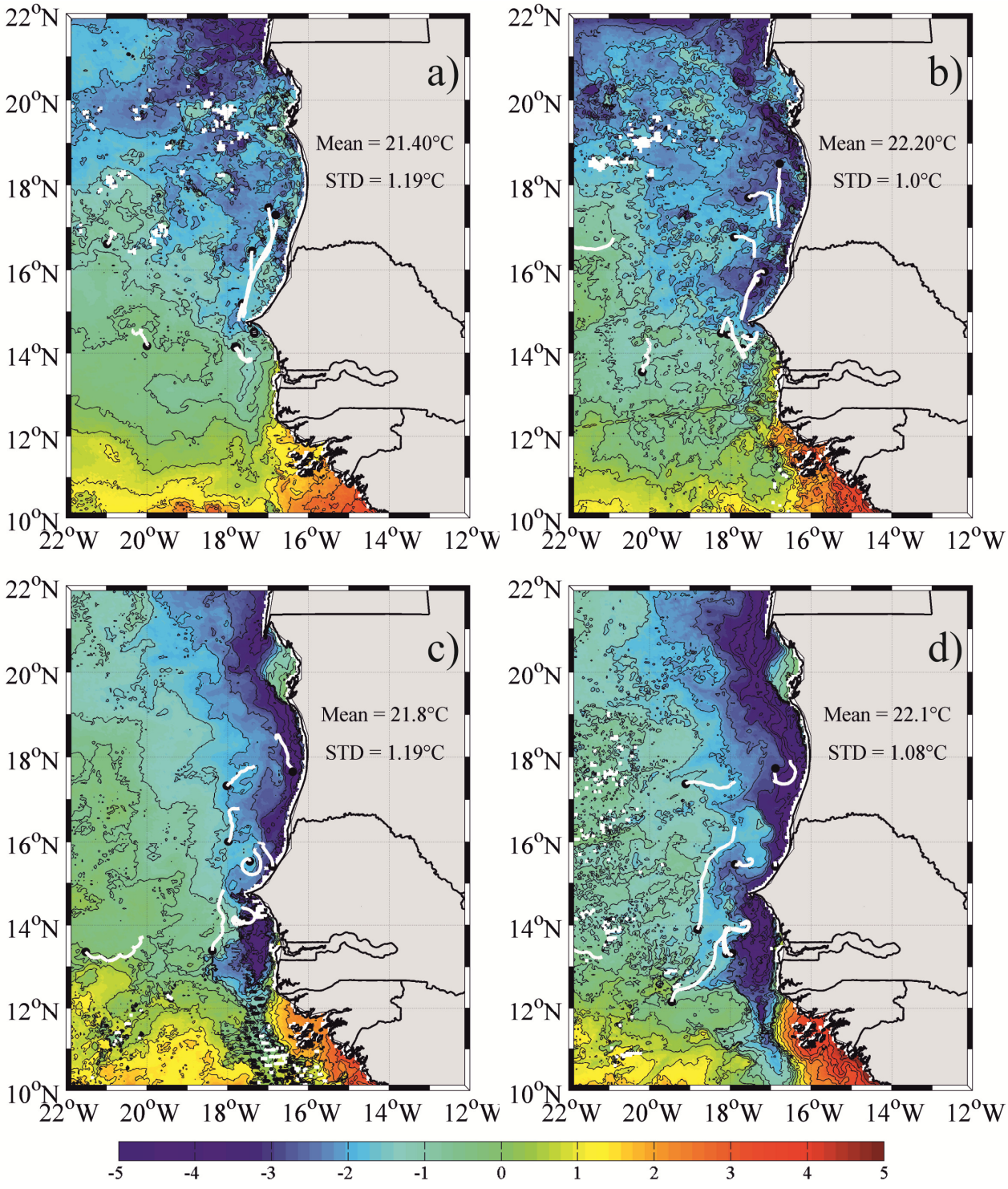

482
483

484 Figure 8
485

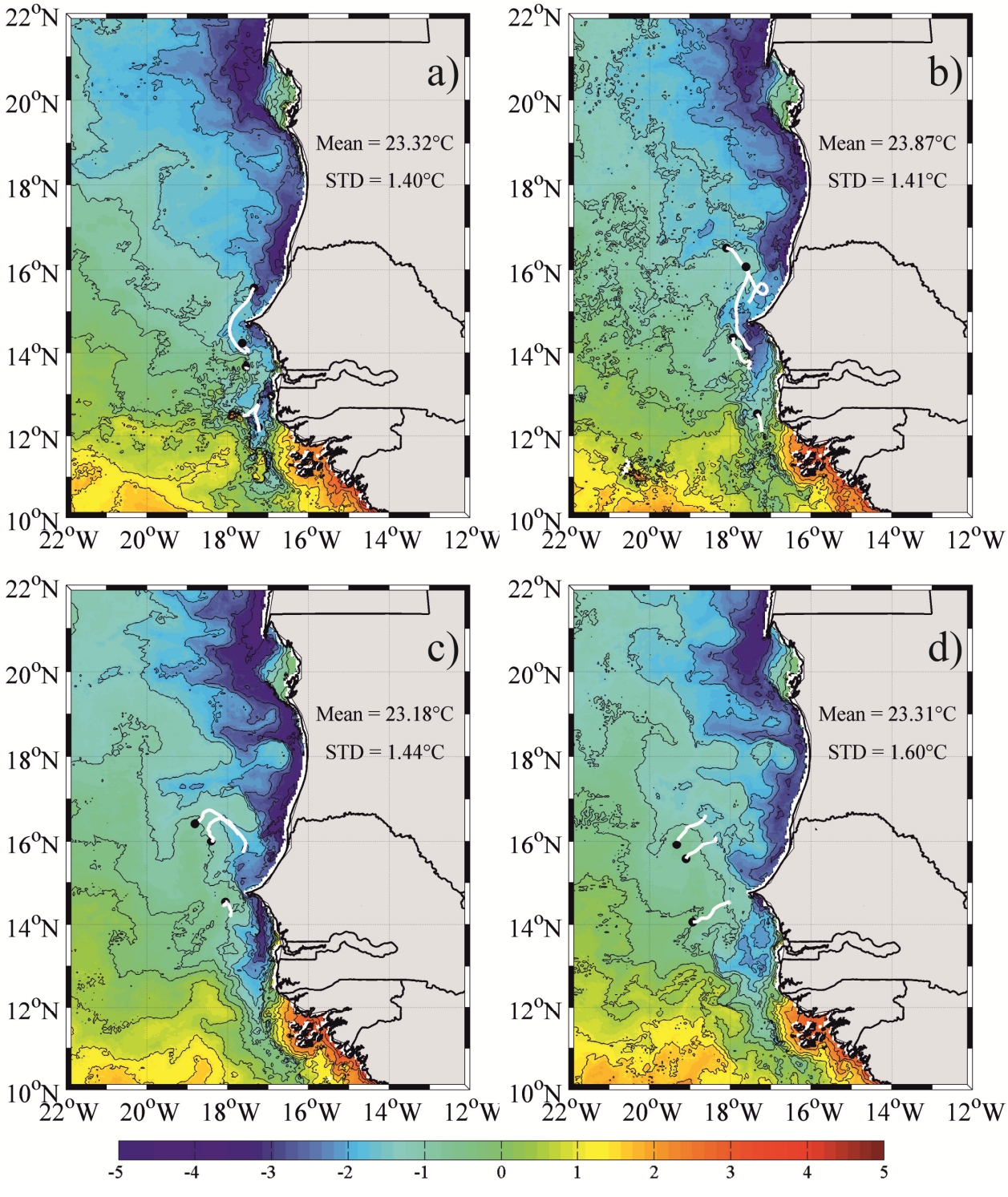

486
487